

Catastrophe Analysis of Structures by Discretization and Modal Transforms*

By

Yoshiji NIWA**, Eiichi WATANABE**, and Hidenori ISAMI**

(Received September 29, 1980)

Abstract

This paper is concerned with the catastrophe of static instability of multi-degree-of-freedom systems representing typical civil engineering structures like beams, columns, arches, plates and stiffened plates.

The proposed method makes use of discretization methods, such as a finite element method and a simplified element method, and also some diffeomorphic transformations similar to modal analysis.

The main interest of the study is the classification of the catastrophe of the structures through the evaluation of certain derivatives of potential in the light of the Thom and Thompsons' theories.

Numerical illustrations were performed on the structures, including elastically supported columns, plates, stiffened plates, lateral buckling of beams and shallow arches. Among new findings, the *unstable symmetric* buckling for lateral buckling, and *hyperbolic umbilics* for the simultaneous buckling of stiffened plates and of elastically supported columns are particularly noted.

Statement of the Problem

As the D.O.F. of structures increases, the possibility of various instability phenomena increases. From the analysts' view point, the instability can be classified into global, partial and local ones, as shown in Table 1. At the same time, engineering structures may be classified in terms of the types of catastrophe or instability [1].

The present paper is particularly concerned with the lower half of this table. The purpose of the study is to see if these marked items are correct, and to find the most influential parameter in each of the items.

In order for the structures to be accounted for by means of discretization methods, a question must be answered regarding whether or not the structure of

* This study has been orally presented at 15th International Congress of Theoretical and Applied Mechanics, Toronto, Canada in August 1980.

** Department of Civil Engineering, Kyoto University, JAPAN

Table 1. Classification of Static Instability of Engineering Structures.

Classification	Name of Structures									
	Stand-Point	Type	Columns	Beams	Arches	Plates	Stiffened Plates	Rigid Frames	Trusses	Shells
View Point		Global	✓	✓	✓			✓	✓	✓
		Partial	✓	✓	✓		✓	✓	✓	✓
		Local	✓	✓	✓	✓	✓			
Types of Instability (CATAS-TROPHE)		Limit Point, Snap-through (<i>FOLD</i>)			✓					✓
		Asymmetric Buckling (<i>FOLD</i>)	✓				✓	✓	✓	✓
		Stable Symmetric (<i>CUSP</i>)	✓	✓		✓	✓	✓	✓	✓
		Unstable Symmetric (<i>DUAL CUSP</i>)	✓	✓	✓	✓	✓	✓	✓	✓

singularities can be realized numerically. To answer this question, either a mathematical argument or an engineering computation will be necessary.

Fujii and Yamaguchi tried to answer the question within the framework of a non-linear operator equation in a Hilbert space, V , by use of the shallow arch and shell theory of von Kármán, Donnell and Marguerre [2]. Then, a numerical approximation of the problem was performed in a class of finite element schemes with the approximate space, V_h . As a concluding remark, it was made clear that the numerical realization of the *cusp* bifurcation in the approximate space, V_h , reveals the imperfections resulting from the use of numerical schemes which are very non-generic, and thus can be avoided.

In the engineering field, however, this question may be equally answered by a comparison of the results such as eigen value, eigen mode, and load-deflection curves from the discretization methods with those from the closed-form solutions, or with those from the experiments concerned.

In the present analysis, either a finite element method with an ACM shape function, or the Simplified Element Method, which one of the authors had developed, was used. The latter method is characterized by the use of linear shape functions, and the use of equivalent elastic springs.

Several results on the normal and unstable behaviour of the engineering structures show that, in general, legitimate use of the finite element method and the simplified element method will surely realize the singularities and instability of the prototype.

Thus, in this paper, discussions will be initiated from those on the elastic and conservative discrete systems.

The analysis can be summarized in the following manner:

a. *Potential, V*

Consider a potential of a discretized model of D.O.F.=N:

$$V: \mathbf{R}^N \times \mathbf{R}^K \rightarrow \mathbf{R},$$

where \mathbf{R}^N refers to a Euclidian behaviour space of dimension N , representing a set of generalized coordinates, w_i ($i=1, \dots, N$); \mathbf{R}^K refers to a K -dimensional Euclidian space, representing the loading and imperfection parameters, p_i ($i=1, \dots, K$).

The equilibrium space, M_V , of this system is given by:

$$M_V = \{(\mathbf{w}, \mathbf{p}) \mid \frac{\partial V}{\partial w_i}(\mathbf{w}, \mathbf{p}) = 0 \quad (i=1, \dots, N)\} \subset \mathbf{R}^N \times \mathbf{R}^K. \quad \dots\dots(1)$$

The catastrophe on this space M_V can be represented by the bifurcation set, Bif χ_V , from a catastrophe map, χ_V :

$$\chi_V: M_V \rightarrow \mathbf{R}^K.$$

b. *Potential, D*

Discussions on the catastrophe using potential V are not realistic since a large D.O.F. is involved. In this paper, the eigen matrix, corresponding to an eigen equation: (See Eqs. (14) & (18))

$$\det [V_{ij}] \equiv \det \left[\frac{\partial^2 V}{\partial w_i \partial w_j} \right] = 0 \quad \dots\dots(2)$$

is used for an Affine transformation h_1 :

$$h_1: \mathbf{R}^n \rightarrow \mathbf{R}^N, \quad \text{or} \quad h_1: \mathbf{v} = (v_1, \dots, v_n) \rightarrow \mathbf{w} = (w_1, \dots, w_N)$$

where

$$1 \leq n \ll N.$$

With respect to the control space, a similar transformation to h_1 can be used for the imperfection parameters, and a translation may be used for the loading parameter:

$$h_2: \mathbf{R}^k \rightarrow \mathbf{R}^K, \quad \text{or} \quad h_2: \mathbf{c} = (c_1, \dots, c_k) \rightarrow \mathbf{p} = (p_1, \dots, p_K)$$

where

$$1 \leq k \ll K.$$

Consider a potential of a discretized model, D , such that

$$D: \mathbf{R}^n \times \mathbf{R}^k \rightarrow \mathbf{R}.$$

Let the equilibrium space be designated by M_D . Then, the catastrophe map, χ_D , can be taken so that

$$\chi_D: M_D \rightarrow \mathbf{R}^k.$$

c. *Potential, A*

Suppose that the corank of Hessian matrix, of potential, D , i.e.,

$$\text{corank } [D_{ij}] \equiv \text{corank } \left[\frac{\partial^2 D}{\partial v_i \partial v_j} \right] = m \quad \dots\dots(3)$$

Since D_{ij} is diagonal, it can be shown after reordering,

$$\begin{aligned} D_{ii} &= 0 \quad (i=1, \dots, m) && (i: \text{not summed}) \\ D_{\alpha\alpha} &\neq 0 \quad (\alpha=m+1, \dots, n) && (\alpha: \text{not summed}) \end{aligned} \quad \dots\dots(4)$$

$(n-m)$ equations of equilibrium, $D_{\alpha} = 0$, will yield the following diffeomorphisms through the theorem of implicit function:

$$v_{\alpha} = g_{\alpha}(v_i, \mathbf{c}) \quad (i=1, \dots, m; \alpha=m+1, \dots, n) \quad \dots\dots(5)$$

Furthermore, consider a map ψ such that

$$\psi: \mathbf{v} = (v_1, \dots, v_n) \rightarrow \mathbf{x} = (v_1, \dots, v_m, v_{m+1} - g_{m+1}, \dots, v_n - g_n) \quad \dots\dots(6)$$

Then, it can be easily shown that the potential function can be written as: [3]

$$D(\mathbf{v}, \mathbf{c}) = (D \circ \psi^{-1})(\mathbf{x}, \mathbf{c}) = A(x_1, \dots, x_m, \mathbf{c}) + \frac{1}{2} \sum_{\alpha=m+1}^n D_{\alpha\alpha} x_{\alpha}^2 \quad \dots\dots(7)$$

This relationship is known as the Splitting Lemma. Potential A can be interpreted as:

$$A: \mathbf{R}^m \times \mathbf{R}^k \rightarrow \mathbf{R},$$

and $A(x_1, \dots, x_m, \mathbf{c})$ represents terms higher than the third order. Variables $x_i = v_i$ ($i=1, \dots, m$) are called *essential variables*, and variables x_{α} ($\alpha=m+1, \dots, n$) are called *unessential variables*.

Let the equilibrium space be designated by M_A . Then, the catastrophe map may be given by χ_A :

$$\chi_A: M_A \rightarrow \mathbf{R}^k.$$

d. *Thom's Potential, F*

When $1 \leq m \leq 2$, $1 \leq k \leq 4$, diffeomorphisms g_1 and g_2 :

$$g_1: \mathbf{R}^m \rightarrow \mathbf{R}^m; \quad g_2: \mathbf{R}^k \rightarrow \mathbf{R}^k$$

will lead to the well-known seven elementary catastrophes by Thom.

The aforementioned discussions may be graphically summarized as follows:

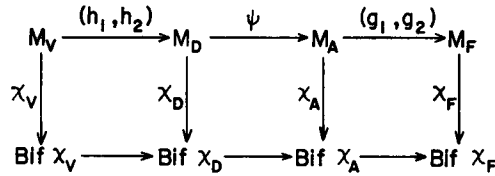


Fig. 1. Relationship among the Four Catastrophe Maps.

In the following sections, detailed discussions on the articles a~c will be provided.

Formulation by Discretization

According to Fujii, the stability problems in non-linear elasticity may be formulated by means of the following non-linear operator equation in a Hilbert space, V : [2]

$$(I - L_\lambda)w + T(w) = \mu \cdot f + g_\lambda \tag{8}$$

where, w refers to the deflections of an arch or shell; L_λ refers to a linear, compact operator, and T a non-linear, continuous compact operator; μ refers to the loading parameter of an assigned lateral load f ; while g_λ refers to a given function of λ , which corresponds to the in-plane force applied to the edge. This equation can be derived from the theory of von Kármán, Donnell and Marguerre.

In the proposed analysis, a discretized model is treated by the displacement method and the so-called Lagrangian formulation.

Let u_i , w_i , P_i^u , and P_i^w denote the nodal in-plane and out-of-plane displacements and the equivalent nodal in-plane and out-of-plane forces, respectively. Moreover, let Q_i^u , Q_i^w , and C_i^w refer to the quadratic pseudo forces in the in-plane and out-of-plane directions, and the cubic pseudo force in the out-of-plane direction, respectively. Then from the principle of virtual work, a set of basic equations of equilibrium can be derived considering the potential, U , in a form similar to the aforementioned non-linear operator equation ($g_\lambda=0$) [4]:

$$\begin{Bmatrix} \frac{\partial U}{\partial u_i} \\ \frac{\partial U}{\partial w_j} \end{Bmatrix} = \begin{Bmatrix} K_{im}^{uu} & K_{in}^{uw} \\ K_{jm}^{wu} & K_{jn}^{ww} \end{Bmatrix} \begin{Bmatrix} u_m^E \\ w_n^E \end{Bmatrix} + \frac{1}{2} \begin{Bmatrix} Q_i^u \\ Q_j^w \end{Bmatrix} + \frac{1}{6} \begin{Bmatrix} 0 \\ C_j^w \end{Bmatrix} - \begin{Bmatrix} P_i^u \\ P_j^w \end{Bmatrix} = \begin{Bmatrix} 0 \\ 0 \end{Bmatrix} \dots (9)$$

where

$$\begin{aligned} K_{im}^{uu} &= K_{im}^p; & K_{in}^{uw} &= K_{ni}^{wu} = K_{inr}^{PB} w_r^I + K_{in}^S \\ K_{jn}^{ww} &= K_{jn}^B + K_{jns}^{BB} w_s^I w_s^I + K_{jnk}^{S} w_k^I + K_{njk}^S w_k^I \end{aligned}$$

and

$$\begin{aligned} Q_i^u &= K_{inr}^{PB} w_n^E w_r^E; \quad Q_j^w = Q_j^{wu} + Q_j^{ww} \\ Q_j^{wu} &= 2K_{mjl}^{PB} u_m^E w_l^E; \quad Q_j^{ww} = 3K_{jnqs}^{BB} w_q^I w_n^E w_s^E + (K_{jnk}^S + K_{njk}^S) w_k^E w_n^E \\ C_j^w &= 3K_{jnqs}^{BB} w_n^E w_q^E w_s^E. \end{aligned} \quad (\text{dummy sum used})$$

Here, the superscripts E , I , P and B refer to the elastic, initial deformations and to the in-plane and out-of-plane stiffnesses, respectively. The superscript S refers to the asymmetric stiffnesses of eccentric stiffeners. Moreover, K_{ij}^P , K_{ij}^B , K_{ij}^S , K_{ijk}^S , K_{ijk}^{PB} and K_{ijkl}^{BB} are constants determined in terms of the geometry of the structure and the mechanical properties. The symmetric stiffnesses of the stiffeners are included in these stiffnesses with the superscripts P and B .

Whether or not the discretization method is legitimate will depend on how and

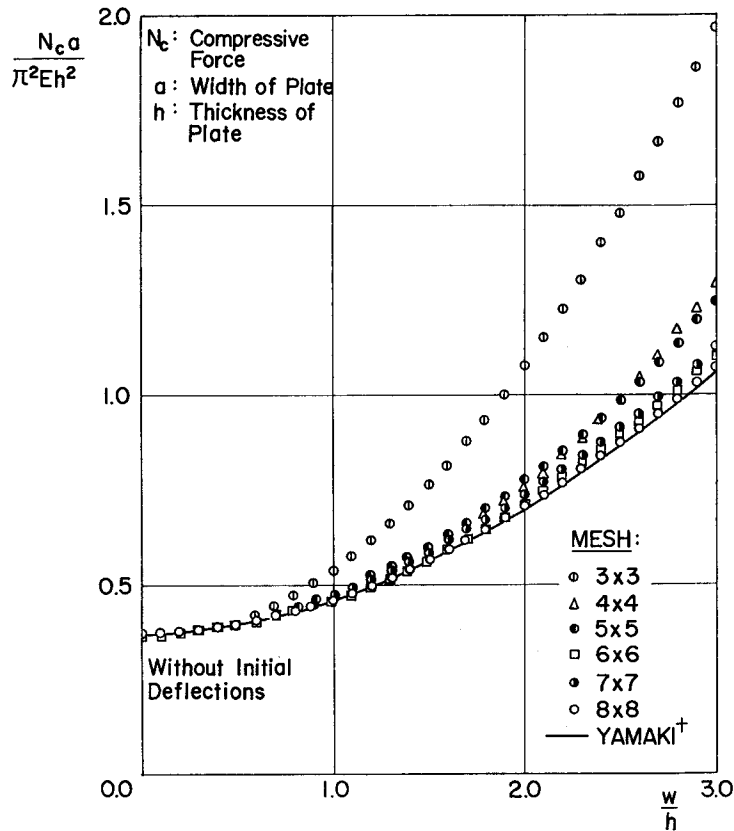


Fig. 2. Load-Deflection Curves at the Central Point of Compressed Square Plates without Initial Deflection. (Under Edge Shortening) $\nu=1/3$. Analyzed by SEM.

† Yamaki, N. : Postbuckling Behaviour of Rectangular Plates with Small Initial Curvature Loaded in Edge Compression, J. Applied Mechanics, Vol. 26, 1959, pp. 407~414.

to what extent the singularities can be realized. Thus, the critical loads, the buckling modes and the load-displacement relationships will serve as a good measure in this respect.

As an example of a legitimate discretization, a flat square plate subjected to in-plane compression is analyzed by the Simplified Element Method [5]. The load-displacement curves are shown in Fig. 2 for initially flat square plates. Here, the effect of the size of mesh is indicated.

Square plates with initial curvatures are also shown in Fig. 3. It may be seen that the results indicate a good numerical realization of the buckling behaviour of plates.

It must be added that the large displacement analyses were performed by a self-correcting perturbation method.

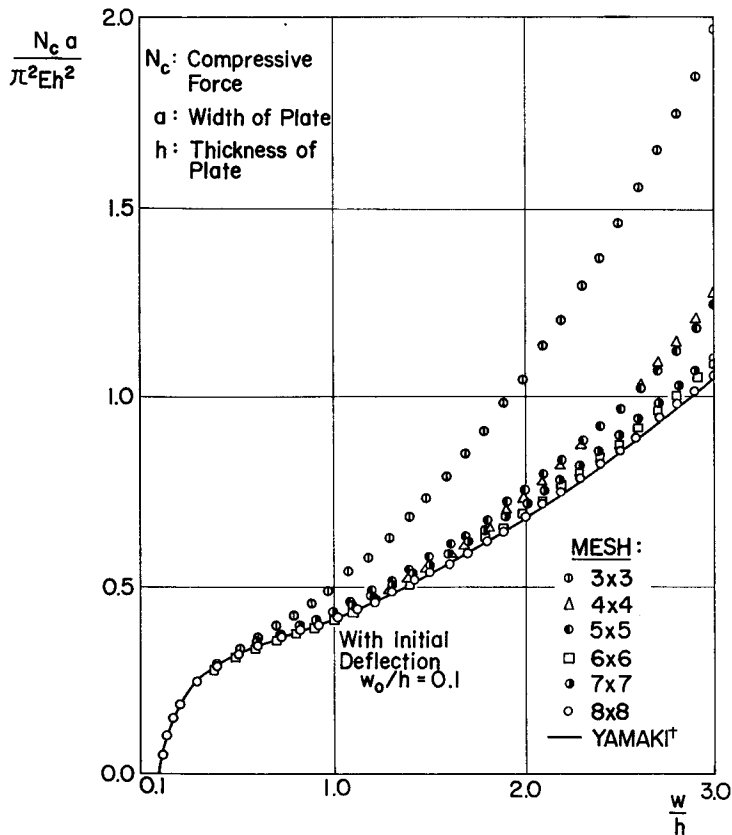


Fig. 3. Load-Deflection Curves at the Central Point of Compressed Square Plates with Initial Deflection. (Under Edge Shortening) $\nu=1/3$. Analyzed by SEM.

Static Condensation

In the derivation of Eq. (9), the non-linearity due to the in-plane displacement was neglected. Thus, the in-plane displacement components can be expressed in terms of the out-of-plane displacement components, namely,

$$u_m^E = A_u (K_{im}^{uu})^{-1} P_{oi}^u - (K_{im}^{uu})^{-1} K_{in}^{uw} w_n^E - \frac{1}{2} (K_{im}^{uu})^{-1} Q_i^u + \lambda_{ui} (K_{im}^{uu})^{-1} \quad \dots\dots(10)$$

in a case where the in-plane nodal forces are prescribed. Here,

$$P_i^u = \lambda_{ui} + A_u P_{oi}^u, \quad \dots\dots(11)$$

and $(K_{im}^{uu})^{-1}$ refers to the inverse matrix of the in-plane stiffness matrix K_{im}^{uu} . Moreover, P_{oi}^u refers to the mode of the in-plane forces prescribed, and λ_{ui} refers to the magnitude of the nodal forces due to the constraint on the displacement component u_i^E .

Let the out-of-plane forces P_j^w be rewritten as

$$P_j^w = A_w P_{oj}^w \quad \dots\dots(12)$$

where P_{oj}^w refers to the mode of the out-of-plane forces.

Then, the potential function mentioned earlier and denoted as V , can be defined after the elimination of the in-plane displacements, u_m^E , in Eq. (10) through Eq. (9) so that

$$V_j(w_i^E, A_u, A_w) = \frac{\partial U}{\partial w_j^E} \quad \dots\dots(13)$$

Here, the suffix j on $V(w_i^E, A_u, A_w)$ indicates a differentiation with respect to w_j^E . Thus,

$$\begin{aligned} V_j = & L_{jn} w_n^E + \frac{1}{2} Q_{jnq} w_n^E w_q^E + \frac{1}{6} C_{jnqs} w_n^E w_q^E w_s^E \\ & - A_w P_{oj}^w + K_{jm}^{wu} (K_{im}^{uu})^{-1} A_u (P_{oi}^u + \lambda_{ui}) = 0 \end{aligned} \quad \dots\dots(14)$$

where

$$\begin{aligned} L_{jn} w_n^E &= (K_{jn}^{ww} - \lambda_{ui} K_{jni}^G - A_u K_{jn}^G - K_{jn}^{www}) w_n^E \\ Q_{jnq} w_n^E w_q^E &= Q_j^{ww} + 2K_{jni}^G K_{iq}^{uw} w_n^E w_q^E - K_{jm}^{wu} (K_{im}^{uu})^{-1} Q_i^u \\ C_{jnqs} w_n^E w_q^E w_s^E &= C_j^w - 3K_{mjn}^{PB} (K_{im}^{uu})^{-1} Q_i^u w_n^E \end{aligned}$$

Again, the form of these equations is similar to that in Eq. (8). In Eq. (14),

$$\begin{aligned} K_{jni}^G &= -K_{mjn}^{PB} (K_{mi}^{uu})^{-1}; \quad K_{jn}^G = K_{jni}^G P_{oi}^u \\ K_{jn}^{www} &= K_{jm}^{wu} (K_{im}^{uu})^{-1} K_{in}^{uw} \end{aligned} \quad \dots\dots(15)$$

In Eq. (14), λ_{ui} vanishes in a case when the in-plane forces are all prescribed. However, it remains unknown otherwise. λ_{ui} can be determined in either of the following cases (It is positive for tensile.):

When $u_p^E = 0$ This situation can be generally found in the case of arches or shells subjected to a lateral loading. The result shows that

$$\lambda_{up} = (F_{kp}^*)^{-1} F_{km} [K_{mn}^{uw} w_n^E + \frac{1}{2} Q_m^u] - A_u P_{op}^u \quad \dots\dots(16)$$

where

$$F_{km} = (K_{mk}^{uu})^{-1} \quad (m=1, \dots, n_u; k=1, \dots, n_c)$$

$$F_{kp}^* = F_{kp} \quad (k=1, \dots, n_c; p=1, \dots, n_c)$$

in which n_u and n_c refer to the in-plane D.O.F. and the number of the constrained in-plane displacements, respectively.

When $u_p^E = f_{pq} u_q$ ($p=1, \dots, n_c; q \neq p$) This situation is generally found in post-buckling analysis of plates and shells when the in-plane displacements are specified along certain edges. Here f_{pq} refers to a prescribed mode of the in-plane displacements along the edges, while q indicates the point free from the constraint. The result will be summarized as follows:

$$\lambda_{up} = (H_{kp}^*)^{-1} H_{km} [K_{mn}^{uw} w_n^E + \frac{1}{2} Q_m^u] - A_u (H_{kp}^*)^{-1} H_{kl} P_{ol}^u - A_u P_{op}^u$$

$$\left. \begin{matrix} \{m=1, \dots, n_u; k=1, \dots, n_c\} \\ \{l=1, \dots, n_u (l \neq p)\} \end{matrix} \right\}$$

where

$$H_{km} = F_{km} - f_{kl} F_{lm} \quad \{m=1, \dots, n_u; k=1, \dots, n_c (l \neq k)\}$$

$$H_{kp}^* = H_{kp} \quad \{k=1, \dots, n_c; p=1, \dots, n_c\} \quad \dots\dots(17)$$

Modal Transforms

From the foregoing discussions, it was found that the equilibrium space, M_v , as defined by Eq. (1), can be explicitly given by Eq. (14). Moreover, the in-plane constraining nodal forces, λ_{up} , were found to be expressed in general by Eq. (17).

Here, however, the considerations will be limited to the cases of $\lambda_{up} = 0$, merely for the sake of simplicity. Later on, in a shallow arch problem, this restriction will be removed.

Now, consider a linear portion of Eq. (14) [6]:

$$(K_{ij}^{ww} - K_{ij}^{uu} - A_u K_{ij}^G) w_j^E = 0 \quad \dots\dots(18)$$

Let Φ_{ij} refer to the eigen matrix†:

† Bathe, K.J.: *Numerical Methods in Finite Element Analysis*, Prentice-Hall, 1976. ... *Subspace Iteration Method*.

$i=1, \dots, N$ ($N=D.O.F.$ for w); $j=1, \dots, n$ ($1 \leq n \leq N$).

Then, it can be shown whether the following transform:

$$w_i = \Phi_{ij} v_j \quad \begin{cases} i=1, \dots, N \\ j=1, \dots, n \end{cases} \quad \dots\dots(19)$$

is diffeomorphic. In order to show this, let us consider a map, $h_1: \mathbf{R}^N \rightarrow \mathbf{R}^N$; $w_i \in \mathbf{R}^N, v_j \in \mathbf{R}^n$ such that

$$\begin{pmatrix} w_1 \\ \vdots \\ w_n \\ w_{n+1} \\ \vdots \\ w_N \end{pmatrix} = \begin{pmatrix} \vdots & \mathbf{0} \\ [\Phi_{ij}] & \vdots \\ \vdots & \vdots \\ \mathbf{0} & 1 \end{pmatrix} \begin{pmatrix} v_1 \\ \vdots \\ v_n \\ 0 \\ \vdots \\ 0 \end{pmatrix} \quad \dots\dots(20)$$

where Φ_{ij} is orthonormalized so that

$$\Phi_{ij} K_{im}^G \Phi_{mk} = \delta_{jk} = \begin{cases} 1 & \text{for } j=k \\ 0 & \text{for } j \neq k \end{cases} \quad \dots\dots(21)$$

$(i, m=1, \dots, N; j, k=1, \dots, n)$

Next, consider another map, $T_1: \mathbf{R}^N \rightarrow \mathbf{R}^N$ such that

$$\begin{pmatrix} v_1 \\ \vdots \\ v_n \\ w_{n+1} \\ \vdots \\ w_N \end{pmatrix} = \begin{pmatrix} [\Phi_{ij}] [K_{ik}^G] & \vdots \\ \vdots & \vdots \\ \mathbf{0} & 1 \end{pmatrix} \begin{pmatrix} w_1 \\ \vdots \\ w_n \\ w_{n+1} \\ \vdots \\ w_N \end{pmatrix} \quad (i=1, \dots, N) \quad \dots\dots(22)$$

Then, in view of Eq. (21), $T_2 = T_1 \cdot h_1$ becomes:

$$T_2 = \begin{pmatrix} 1 & 1 & \mathbf{0} & \Phi_{i1} K_{i,n+1}^G, \dots, \Phi_{i1} K_{i,N}^G \\ & \ddots & & \vdots \\ & \mathbf{0} & 1 & \vdots \\ & & & \vdots \\ \hline \Phi_{n+1,1} \dots \Phi_{n+1,n} & 1 & & \mathbf{0} \\ \vdots & & \ddots & \vdots \\ \Phi_{N,1} \dots \Phi_{N,n} & \mathbf{0} & & 1 \end{pmatrix} \quad \dots\dots(23)$$

It is obvious that $\det T_2$ is unity whenever $n=N$.

Now, provided that

$$\det T_2 = \det T_1 \cdot \det h_1 = \det (\Phi_{ij} K_{ik}^G \Phi_{kl}) \neq 0, \quad \dots\dots(24)$$

$\begin{pmatrix} i=1, \dots, N \\ j, k, l=1, \dots, n \end{pmatrix}$

then,

$\det h_1 \neq 0$ and $\det T_1 \neq 0$.

In this case, mapping h_1 is shown to be one-to-one correspondent and diffeomorphic.

Let v_i^I designate the generalized initial displacements transformed through Eq. (19) from w_j^I . Then, the following transformation can be made with respect to the control space:

$$h_2: \mathbf{c} = (c_1, \dots, c_k) \rightarrow \mathbf{p} = (p_1, \dots, p_K)$$

where

$$\begin{aligned} c_1 &= A_u; c_2 = v_1^I, \dots, c_k = v_n^I \\ p_1 &= A_u; p_2 = w_1^I, \dots, p_K = w_K^I \end{aligned} \quad \dots\dots(25)$$

and

$$k = n+1; K = N+1$$

Now, let us define a new potential D so that

$$D(v_i^E, \mathbf{c}) = V(w_j^E, \mathbf{p}) \quad \dots\dots(26)$$

Through Eq. (19), the first partial differentiation of D with respect to v_i^E yields:

$$D_i \equiv \frac{\partial D}{\partial v_i^E} = V_j \Phi_{ji} = 0^\dagger \quad \dots\dots(27)$$

The explicit form of D_i is given by the product of the right hand side of Eq. (14) and Φ_{ji} , where \mathbf{w} has been expressed in terms of \mathbf{v} , by Eq. (19).

Potential in Terms of Essential Variables

Let the corank of the Hessian matrix D_{ij} be m . In other words, let us assume an m -fold coincident buckling.^{††} Then, from Eq. (3) and the implicit function theorem, it has been shown that the unessential modes, v_α ($\alpha=m+1, \dots, n$), can be expressed in terms of the control parameters and the essential modes, v_i ($i=1, \dots, m$), in the form of Eq. (4), after some reordering.

Upon substitution of these expressions into Eq. (27), a new potential, A , can be defined through the implicit function theorem by the following equation.

$$A(v_i, \mathbf{c}) = D[v_i, v_\beta(v_j, \mathbf{c}), \mathbf{c}] \quad \dots\dots(28)$$

where the Roman and Greek subscripts on v refer to the active and passive modes, or in other words, the essential and unessential modes, respectively.

The substitution of Eq. (28) into the equilibrium equations, $D_\alpha=0$, will yield

[†] This is equivalent to obtaining the orthogonal projection in Euclid space \mathbf{R}^n .

^{††} In other words, $\dim \ker (I-L_\lambda)=m$ in Eq. (8).

the identities:

$$D_{\alpha}[v_i, v_{\beta}(v_j, \mathbf{c}), \mathbf{c}] = 0 \quad \dots\dots(29)$$

The left-hand side now represents a function of totally $(m+k)$ independent variables. Thus, it can be differentiated as many times as desired. Thus,

$$\begin{aligned} \frac{\partial D_{\alpha}}{\partial v_i} &= D_{\alpha i} + D_{\alpha\beta} v_{\beta,i} = 0 \\ \frac{\partial D_{\alpha}}{\partial A_u} &= D_{\alpha\beta} v'_{\beta} + D'_{\alpha} = 0 \end{aligned} \quad \dots\dots(30)$$

where $v_{\beta,i} \equiv \frac{\partial v_{\beta}}{\partial v_i}$; $v'_{\beta} \equiv \frac{\partial v_{\beta}}{\partial A_u}$

Since $D_{\alpha\beta} = 0$ for $\alpha \neq \beta$
 $= D_{\alpha\alpha} \neq 0$ for $\alpha = \beta$,

the following important relationships can be easily obtained:

$$\begin{aligned} v_{\alpha,i} &= -D_{\alpha i} / D_{\alpha\alpha} = 0 \quad (\alpha: \text{not summed}) \\ v'_{\alpha} &= -D'_{\alpha} / D_{\alpha\alpha} \quad (\alpha: \text{not summed}) \\ v_{\alpha,ij} &= -D_{\alpha ij} / D_{\alpha\alpha} \quad (\alpha: \text{not summed}) \\ A_i &\equiv \frac{\partial A}{\partial v_i} = 0 \\ A_{ij} &= D_{ij} \\ A_{ijk} &= D_{ijk} \\ A_{ijkl} &= D_{ijkl} - \sum_{\alpha} (D_{ij\alpha} D_{kl\alpha} + D_{ik\alpha} D_{jl\alpha} + D_{il\alpha} D_{jk\alpha}) / D_{\alpha\alpha} \\ A' &= D' \\ A'' &= D'' \\ A'_i &\equiv \frac{\partial^2 A}{\partial A_u \partial v_i} = D'_i \end{aligned} \quad \dots\dots(31)$$

Numerical Illustrations

Several numerical illustrations were performed to find the catastrophe characteristics by use of Eq. (31).

Elastically Supported Column Fig. 4 shows a column simply supported at one end and elastically supported at the other end. The analysis was performed using both FEM (ACM shape function) and the Simplified Element Method (abbreviated as SEM). The results are shown in Table 2. The catastrophe is seen depending on the value of $\kappa = \pi^2 EI / (KL^3)$:

i.e. when $\kappa > 0.5 \dots$ fold

$\kappa = 0.5 \dots$ hyperbolic umbilic

$\kappa < 0.5 \dots$ dual cusp

The FEM analysis using an ACM shape function was found to overestimate the postbuckling strength of the columns, and the values of D_{1111} and A_{1111} .

Table 2. Stability of Asymmetric Buckling Model of Columns.

			16 Elements		32 Elements	
			SEM	FEM	SEM	FEM
$\kappa = 0.25$: DUAL CUSP	$\frac{A_{cr}L^2}{\pi^2EI}$	1st	0.9978	1.0010	1.0002	1.0010
		2nd	2.0010	2.0010	2.0010	2.0010
	Mode	1st	a*	a	a	a
		2nd	b	b	b	b
	D_{112c}^{**}		-0.005	-0.005	-0.005	-0.005
	D_{222c}		-0.002	-0.002	-0.002	-0.002
	$D_{22c} \times 10^3$		0.5150	0.5132	0.5112	0.5112
	D_{1111c}		0.0747	0.6537	0.0749	0.6419
	A_{1111c}		-0.074	0.503	-0.0676	0.491
	$\kappa = 0.5$: HYPERBOLIC UMBILIC	$\frac{A_{cr}L^2}{\pi^2EI}$	1st	1.0003	0.9973	1.0003
2nd			1.0005	1.0003	1.0005	1.0003
Mode		1st	b	a	b	a
		2nd	a	b	a	b
$10^3 \times D_{111c}$		0.7697	0.0	0.7697	0.0	
$10^2 \times D_{112c}$		0.0	0.2537	0.0	0.2533	
$10^2 \times D_{221c}$		0.2535	0.0	0.2535	0.0	
$10^3 \times D_{222c}$		0.0	0.7697	0.0	0.7697	
$\frac{2A'_{11c}}{A_{22c}} - \frac{A_{111c}}{A_{122c}}$ ⁷⁾		0.1016	—	0.1016	—	
$\frac{2A'_{22c}}{A_{11c}} - \frac{A_{222c}}{A_{211c}}$		—	0.1019	—	0.1017	
$\kappa = 0.75$: FOLD	$\frac{A_{cr}L^2}{\pi^2EI}$	1st	0.6668	0.6668	0.6668	0.6668
		2nd	0.9971	1.0004	0.9995	1.0004
	Mode	1st	b	b	b	b
		2nd	a	a	a	a
	$10^3 \times D_{111c}^{***}$		0.5134	0.5134	0.5134	0.5134
	$10^2 \times D_{122c}$		0.1685	0.1691	0.1689	0.1691

* Mode a:  b: 

** Suffix c refers to the evaluation at the lowest critical load.

*** For single-degree-of-freedom system, this is 0.5140. D_{22} , D_{111} , D_{1111} are non-dimensionalized by $L|EA$, $L^2|EA$, $L^3|EA$, respectively and so on.

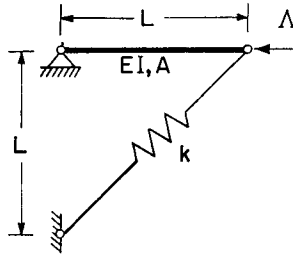


Fig. 4. Asymmetric Buckling Model of Columns.

Compressed Square Plates The square plates are subjected to uniformly distributed axial compressive stress. The unloaded edges are free from in-plane constraints. Moreover, the plates are all simply supported, and the Poisson's ratio is $1/3$. The results are given in Table 3.

Table 3. Stability of Compressed Simply Supported Square Plates.
 $\nu=1/3$. Analyzed by SEM.

	3×3	4×4	5×5	6×6	7×7	8×8
k_1^* (1st)	3.830	3.901	3.936	3.955	3.967	3.975
k_2 (2nd)	4.742	5.326	5.635	5.814	5.926	6.000
K_{iiii}^{BB**}	197.1	77.3	127.8	90.5	114.6	95.6
K_{iiii}^{BPB**}	162.9	66.6	111.7	79.6	101.2	84.7
A_{iiii}^{**}	34.2	10.7	16.1	10.9	13.3	10.9

* k_1 and k_2 refer to the buckling coefficients.

** All non-dimensionalized by the factor of b^2/Eh . b, h refers to the width & thickness of the square plates, respectively. (Fig. 5)

The result shows that the catastrophe is a *cuspl*. When the in-plane displacements are constrained, the stability is generally improved.

Square Stiffened Plates The stiffened square plates are subjected to uniformly distributed axial compressive stress. The support condition is all simply supported, and is eccentrically spliced to the plate.

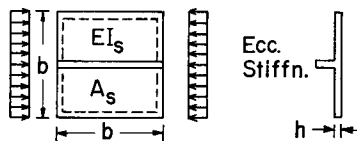


Fig. 5. Compressed Stiffened Square Plates.

In this model, the stiffnesses such as K_{ij}^S , and K_{ijk}^S in Eq. (9) play an important role.

The results are shown in Table 4 for different combinations of the following

typical parameters of stiffened plates.

$$\gamma = \frac{EI_s^\dagger}{bD}; \quad \delta = \frac{A_s}{bh}$$

Table 4. Stability of Stiffened Square Plates.

	Case-1	Case-2	Case-3	Case-4
$\gamma = EI_s/bD$	5.0	14.75	14.80	20.0
$\delta = A_s/bh$	0.1	0.1	0.1	0.1
k_1 (1st)	4.314	14.295	14.295	14.295
k_2 (2nd)	10.455	14.295	14.296	14.300
A_{111c}^*	12.44	356.22	260.30	521.63
A_{222c}^*	87.78	396.96	253.40	504.20
A_{111c}^{**}	0.1252	-0.012	-0.003	-0.124×10^{-5}
A_{122c}^{**}	-0.022	-0.2328	-0.0012	-0.662×10^{-6}
A_{222c}^{**}	-0.0161	0.942×10^{-3}	0.0047	0.0016
A_{112c}^{**}	0.0687	0.405×10^{-3}	0.0016	0.372×10^{-6}
$\frac{2A'_{11c}}{A'_{22c}} - \frac{A_{111c}}{A_{122c}} \text{ ?}$	—	-1.323	-0.478	—
$\frac{2A'_{22c}}{A'_{11c}} - \frac{A_{222c}}{A_{111c}}$	—	-0.236	-0.959	—
$A_{111c} \cdot A_{122c}$	—	Positive	Positive	—
$A_{222c} \cdot A_{112c}$	—	Positive	Positive	—
Type of Buckling	ASYMM.	MONO-CLINAL	MONO-CLINAL	STABLE SYMM.
Catastroph	FOLD	HYPERB. UMBILIC	HYPERB. UMBILIC	CUSP

* Non-dimensionalized by b^2/Eh . ** Non-dimensionalized by b/Eh .

The analysis was performed by SEM.

Lateral Buckling Fig. 6 shows plates subjected to a concentrated in-plane load.

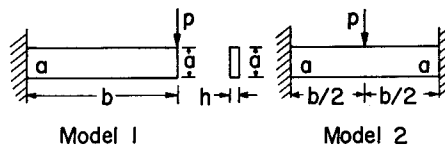


Fig. 6. Lateral Buckling Model. $\nu=0.3$.

The analysis was made by FEM with an ACM shape function. The result of the analysis is shown in Table 5.

$\dagger D = Eh^3/[12(1-\nu^2)]$ (ν : poisson's ratio)

Table 5. Stability of Lateral Buckling.

	b/a	DOF		Mode $i=1$	Mode $i=2$
Model 1	8	80	$\frac{P_{cr}b}{\pi^2 D}$	0.0687	-0.0793
			$\frac{b^2 A_{iiii}}{Eh}$	-3.013	-3.294
Model 1	4	40	$\frac{P_{cr}b}{\pi^2 D}$	0.1361	-0.1787
			$\frac{b^2 A_{iiii}}{Eh}$	-2.395	-3.198
Model 2	8	70	$\frac{P_{cr}b}{\pi^2 D}$	0.6292	1.2759
			$\frac{b^2 A_{iiii}}{Eh}$	-4.016	-2.479

Thus, the catastrophe is estimated to be a *dual cusp*.

Stability of Shallow Arch

Fig. 7 shows an example of the shallow arches for analysis.

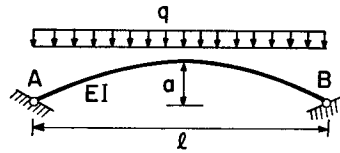


Fig. 7. Two-Hinged Arch.

The arch is assumed to be subjected to a uniform lateral load. This structure is also assumed to be as a beam-column with an initial curvature.

From Eqs. (9), (14)~(16), the equations of equilibrium can be written as

$$\begin{aligned}
 V_j = & [K_{jn}^B + (K_{jnkl}^{BB} - K_{jnkl}^{BPB})w_k^I w_l^I - \lambda_p K_{jn}^G]w_n^E \\
 & + \frac{1}{2}(K_{jnkl}^{BB} - K_{jnkl}^{BPB})^*(3w_n^E w_k^E w_l^I - w_n^E w_k^E w_l^E) \\
 & - A_w P_{oj}^w - \lambda_p K_{jn}^G w_n^I \quad \dots\dots(32)
 \end{aligned}$$

The horizontal thrust, λ_p , acting at ends A and B in Fig. 7, can be given by:

$$\lambda_p = -(F_{kp}^*)^{-1} F_{km} K_{mnr}^{PB} (w_r^I + \frac{1}{2} w_r^E) w_n^E \quad \dots\dots(33)$$

where

$$K_{jnkl}^{BPB} = K_{ijn}^P (K_{im}^P)^{-1} K_{mkl}^{PB} \quad \dots\dots(34)$$

In Eq. (33), the suffix p refers to the ends of the arch, i.e., either point A or B .

In order to make a catastrophe analysis, Eq. (32) must be condensed in some appropriate manner. Let us again make use of an Affine transform as given by Eq. (19). However, this time, the modal matrix $[\Phi_{ij}]$ will be obtained from the eigen value problem of the corresponding column:

$$(K_{ij}^B - \lambda_p K_{ij}^G)w_j = 0 \quad \dots\dots(35)$$

Then, the condensed equations of equilibrium can be written in the form:

$$D_i = \Phi_{ij}V_j = [K_{im}^B + K_{imni}v_n^I v_i^I - \lambda_p K_{im}^G]v_m^E + \frac{1}{2} K_{imkn}(3v_m^E v_k^E v_n^I - v_m^E v_k^E v_n^E) - A_w \bar{P}_{oi}^w - \lambda_p K_{im}^G v_m^I \quad \dots\dots(36)$$

where

$$\begin{aligned} K_{im}^B &= \Phi_{ji} K_{jn}^B \Phi_{nm}; & K_{im}^G &= \Phi_{ji} K_{jn}^G \Phi_{nm} \\ K_{imkn} &= (K_{j\ p\ q\ r}^{BB} - K_{j\ p\ q\ r}^{BPB}) \Phi_{ji} \Phi_{pm} \Phi_{qn} \Phi_{rn} \\ \bar{P}_{oi}^w &= \Phi_{ji} P_{oj}^w \end{aligned} \quad \dots\dots(37)$$

and

$$\begin{aligned} \lambda_p &= -\bar{c}_{ij} \left(v_i^I + \frac{1}{2} v_i^E \right) v_j^E \\ \bar{c}_{ij} &= (F_{kp}^*)^{-1} F_{km} K_{mnr}^{PB} \Phi_{ni} \Phi_{rj} \end{aligned} \quad \dots\dots(38)$$

Since the terms involving K_{imkn} are very small in the case of columns, the following simplified equations are derived. Let v_1 and v_2 designate the generalized displacement corresponding to the mode of snap-through and bifurcation buckling, respectively. Then†,

$$-\lambda_p = \frac{1}{2} \bar{c}_{11}(v_1^E + v_1^I)^2 + \frac{1}{2} \bar{c}_{22}v_2^E{}^2 - \frac{1}{2} \bar{c}_{11}v_1^I{}^2 \quad \dots\dots(39)$$

The equations of equilibrium are given by

$$\begin{aligned} D_1 &= K_{11}^B v_1^E - \lambda_p K_{11}^G (v_1^I + v_1^E) - A_w \bar{P}_{o1}^w = 0 \\ D_2 &= K_{22}^B v_2^E - \lambda_p K_{22}^G v_2^E = 0 \end{aligned} \quad \dots\dots(40)$$

Furthermore, the 2nd derivatives of D are

$$\begin{aligned} D_{11} &= K_{11}^B - \frac{1}{2} \bar{c}_{11}v_1^I{}^2 + \frac{3}{2} \bar{c}_{11}(v_1^I + v_1^E)^2 + \frac{1}{2} \bar{c}_{22}v_2^E{}^2 \\ D_{22} &= K_{22}^B - \frac{1}{2} \bar{c}_{11}v_1^I{}^2 + \frac{1}{2} \bar{c}_{11}(v_1^I + v_1^E)^2 + \frac{3}{2} \bar{c}_{22}v_2^E{}^2 \end{aligned} \quad \dots\dots(41)$$

The postbuckling path can be obtained from Eq. (40);

† $K_{11}^G = K_{22}^G = 1, K_{12}^G = 0; \bar{c}_{12} = 0, \bar{c}_{11} = \bar{c}_{22} = \bar{c}$

$$(\bar{K}_{11}^B - \bar{K}_{22}^B)v_1^E - \bar{K}_{22}v_1^I = A_w \bar{P}_{o1}^w \quad \dots\dots(32)$$

Furthermore, it can be shown that

$$\begin{aligned} D_1' &= \partial D_1 / \partial A_w = -\bar{P}_{o1}^w \neq 0 \\ D_{111} &= 3\bar{\sigma}_{11}(v_1^I + v_1^E) \neq 0 \end{aligned} \quad \dots\dots(43)$$

at the load corresponding to $D_{11}=0$. Thus, the point $D_{11}=0$ will be found to be a *Limit Point*, or a *Fold Catastrophe*.

On the other hand, at point $D_{22}=0$, v_2^E is likewise zero, and

$$A_{2222} = D_{2222} - 3D_{221}^2/D_{11} = -3 \frac{\bar{K}_{22}^B - \bar{K}_{11}^B}{\bar{\sigma}_{11}v_1^{I2} + \bar{K}_{11}^B - 3\bar{K}_{22}^B} \bar{\sigma}_{11} < 0 \quad \dots\dots(44)$$

Thus, the point $D_{22}=0$ will be found to be an *Unstable Symmetric Buckling Point*, or a *Dual Cusp Catastrophe*.

The snap-through load, $(A_w)_{SNT}$, can be obtained as

$$-(A_w)_{SNT} \bar{P}_{o1}^w = \frac{\bar{\sigma}_{11}}{3\sqrt{3}} \left(v_1^{I2} - \frac{2\bar{K}_{11}^B}{\bar{\sigma}_{11}} \right)^{3/2} + \bar{K}_{11}^B v_1^I. \quad \dots\dots(45)$$

or written in Timoshenko's form†:

$$u = 1 + \sqrt{\frac{4}{27} (1 - \bar{m})^3 / \bar{m}^2}$$

where

$$\begin{aligned} u &= -(A_w)_{SNT} \bar{P}_{o1}^w / (\bar{K}_{11}^B v_1^I) \dagger\dagger \\ \bar{m} &= 2\bar{K}_{11}^B / (\bar{\sigma}_{11} v_1^{I2}) \dagger\dagger\dagger \end{aligned}$$

The stability of the arch treated herein may thus be classified in terms of the rise of the arch, v_1^I , in the manner shown in Fig. 8:

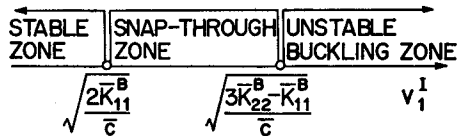


Fig. 8. Stability of Shallow Arch.

The curves of the snap-through and the bifurcation buckling are given in Fig. 9. Here, the solid and broken lines indicate the stable and unstable paths,

† Timoshenko & Gere: *Theory of Elastic Stability*, McGraw-Hill, 2nd ed., 1961.
 †† Very close to $5ql^4/(384EIa)$.
 ††† Very close to $4I/(Aa^2)$.

respectively.

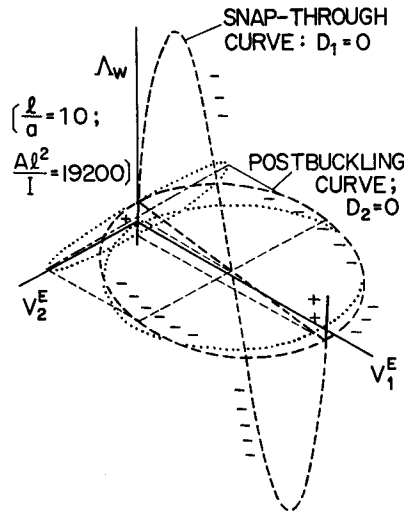


Fig. 9. Equilibrium Paths of a Shallow Arch.
 $v_1^l > \sqrt{(3K_{22}^B - K_{11}^B)/\bar{c}}$.

Convergence of Derivatives

The classification of the stability depends on the evaluation of the potential derivatives, such as A_{ijk} and A_{ijkl} . The results of the numerical analysis showed that the 3rd order derivatives, A_{ijk} , converge very rapidly with respect to the number of meshes.

On the other hand, the computation of the 4th order derivatives, A_{ijkl} , is an extremely time-consuming process. Particularly, the evaluation of the condensed K_{ijkl}^{BPPB} (See Eq. (34)) needs much computation time. As a matter of fact, this is why SEM should be conveniently used rather than FEM: The evaluation of K_{ijkl}^{BPPB} by FEM would be astonishingly costly. Therefore, most of the convergence checks were performed by SEM.

Fig. 10 shows the convergence of K_{1111}^{BB} and K_{1111}^{BPPB} :

$$K_{1111}^{BB} = K_{ijkl}^{BB} \Phi_{i1} \Phi_{j1} \Phi_{k1} \Phi_{l1}$$

$$K_{1111}^{BPPB} = K_{ijkl}^{BPPB} \Phi_{i1} \Phi_{j1} \Phi_{k1} \Phi_{l1}$$

for simply supported columns with respect to the number of elements employed in the SEM analysis. From Fig. 10, these coefficients will be seen to have converged well.

Fig. 11 shows simply supported square plates subjected to uniformly distributed

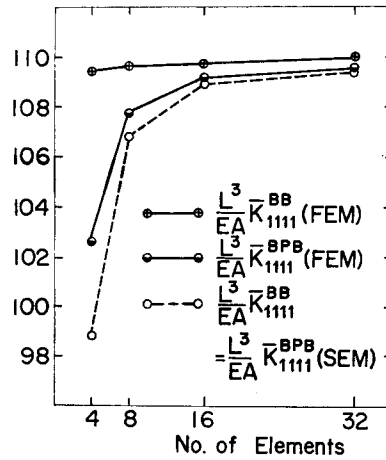


Fig. 10. Convergence of K_{1111}^{BB} and K_{1111}^{BPB} for Clumns. Analyzed by SEM and FEM.

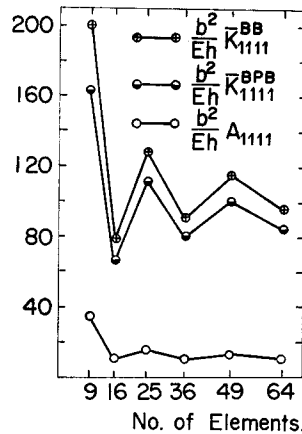


Fig. 11. Convergence of 4th Derivatives for Simply Supported Square Plates under Uniformly Distributed Axial Compression. $\nu=1/3$. Analyzed by SEM.

axial compressive stress, where the unloaded edges are free from in-plane constraints. The results will again show a good convergence. (Analysis made by SEM.)

Conclusions

The main conclusions include the following:

1. The lateral buckling of beams is controlled by an *unstable symmetric buckling*, or a *dual cusp*.
2. The compressed stiffened plates with an eccentric stiffener are subjected to a

hyperbolic umbilic catastrophe, or a *monoclinal buckling* when the simultaneous buckling occurs. This will strengthen Thompson and Hunts' results on infinitely wide stiffened plates [7].

3. The columns supported with an inclined spring at one end and simply supported at the other end will be subjected to an *asymmetric buckling*, or a *fold catastrophe* when the spring constant is relatively small, to an *unstable symmetric buckling*, or a *dual cusp catastrophe* when the constant is sufficiently large and a *hyperbolic umbilic catastrophe*, or a *homeoclinical buckling* when the constant takes a particular value.

4. The stability of plates subjected to the in-plane loading depends largely on whether they are subjected to a forced in-plane displacement along a boundary, or to the loading prescribed along the boundary. The results show that the former case is more stable.

5. The physical interpretations of the discretization methods and modal transforms were provided.

6. A shallow arch was analyzed by assuming that it can be represented as a beam-column with an initial curvature. Here again, the catastrophe was found to be either a *fold* or a *dual cusp* according to the magnitude of the rise of the arch.

This study accepted a Grant-in-Aid for Scientific Research from the Ministry of Education in the years of 1978 and 1979.

Bibliography

- 1) Thompson, J.M.T. and G.W. Hunt: A General Theory of Elastic Stability, John Wiley and Sons, 1973.
- 2) Fujii, H. and M. Yamaguchi: Simple Buckling — A Group Theoretical Introduction —, Report of Study on the Theory and Numerical Analysis on Stability, Bifurcation, and Buckling in Non-linear Theory of Elasticity. Research Institute for Mathematical Sciences, Kyoto University, 1979.
- 3) Poston, T. and I. Stewart: Catastrophe Theory and its Applications, Pitman, 1978.
- 4) Watanabe, E. and Y. Yamada: On the Behaviour and Ultimate Strength of Longitudinally Stiffened Flanges of Steel Box Girders, Proc. of JSCE, No. 252, 1976, pp. 127-142.
- 5) Watanabe, E. and Y. Yamada: Compressive Strength of Plates with Closed-sectional Ribs, Proc. of JSCE, No. 278, 1978, pp. 133-147.
- 6) Niwa, Y., E. Watanabe, and H. Isami: Catastrophe and Load-Carrying Capacity of Structures, 28th Congress on Theoretical and Applied Mechanics, 515(A), 1978.
- 7) Thompson, J.M.T. and G.W. Hunt: Towards a Unified Bifurcation Theory, ZAMP, Vol. 26, 1975, pp. 581-603.